THE ASTROPHYSICAL JOURNAL, 516:9–17, 1999 May 1
© 1999. The American Astronomical Society. All rights reserved. Printed in U.S.A.

RADIO-QUIET RED QUASARS

DONG-WOO KIM[1]
Chungnam National University, Taejon, 305-764, South Korea
AND
MARTIN ELVIS
Harvard-Smithsonian Center for Astrophysics, 60 Garden Street, Cambridge, MA 02138
Received 1998 May 11; accepted 1998 December 8

ABSTRACT

We have performed a successful targeted search for a population of red, radio-quiet, and probably absorbed quasars. Radio-quiet, optically red *ROSAT* PSPC X-ray sources brighter than 1×10^{-13} ergs cm^{-2} s^{-1} were searched for red ($O-E > 2.0$, $O \leq 20$) counterparts in the Automated Plate-measuring Machine catalog of Palomar Sky Survey objects. Of 45 objects for which we obtained adequate follow-up optical spectroscopy, we have found seven red quasars, five with $\alpha_{\rm opt} < -2$. Their redshifts range from 0.06 to 0.31, and their luminosities are moderate, lying on the quasar/Seyfert boundary. These red quasars strengthen the case for a radio-quiet population that is the counterpart of the radio-loud red quasars found by Smith & Spinrad and Webster et al. Unidentified, fainter sources could increase the fraction of red quasars by up to a factor of 7. For the red quasars found here, the Hα/Hβ ratios, optical slope, and X-ray colors all indicate that they are absorbed by $A_V \sim 2$ rather than having intrinsically red spectra. This amount of obscuration seems to hide $\sim$1%–7% of quasars at a given observed flux or $\sim$3%–20% when their fluxes are corrected to their intrinsic values. This size of population is consistent with earlier limits, with predicted values from Comastri et al., and is comparable with the rate found among radio-loud quasars. A large population of more heavily absorbed ($A_V = 5$), fainter quasars equal in size to the blue population could exist without violating existing upper limits, which is in accord with the Comastri et al. predictions.

Subject headings: dust, extinction — quasars: general — X-rays: galaxies

1. INTRODUCTION

Quasars are the canonical "ultraviolet excess" objects (Sandage 1965). Yet red quasars have been found in radio-selected samples by Smith & Spinrad (1980) and Webster et al. (1995). Webster et al. (1995) proposed that a large fraction, perhaps 80%, of radio-loud quasars might have been hidden as red objects. Moreover, the currently favored explanations for the cosmic X-ray background invoke a population of heavily obscured active galactic nuclei (AGNs) 5 times more common than the unobscured population (Comastri et al. 1995). If the small number of known red quasars really is the "tip of the iceberg" of a large, even dominant, quasar population, then the consequences would be interesting: the overall AGN population—and so the massive black hole population—may be 5 times larger than had been thought; obscured quasars would be a long-lived evolutionary phase (see Sanders et al. 1988), or all quasars may be hidden along 80% of possible lines of sight; and red quasars may contribute importantly to the cosmic X-ray background. The Webster et al. conclusion is widely disputed. Boyle & di Matteo (1995), Stickel et al. (1996), and Benn et al. (1998) all argue that any missing population must be smaller and perhaps insignificant, while Gunn & Shanks (1998) disagree. Here we present an X-ray–based survey targeted explicitly at red AGNs to find radio-quiet red quasars.

Radio-loud red quasars are relatively easy to find, since the radio emission is unaffected by absorbing gas or dust and, in low-frequency surveys, usually comes from the large radio lobes that lie well outside any obscuring material in the host galaxy. An explicit, albeit small-scale, search for radio- and X-ray–loud but optically quiet quasars, which should include reddened quasars, was, however, not successful (Kollgaard et al. 1995).

Radio-quiet red quasars are much harder to find, although they might be expected to be much more common. In the normal unreddened population, radio-quiet quasars outnumber radio-loud quasars 10 to 1 (e.g., the Extended Medium Sensitivity Survey, Stocke et al. 1991; the Palomar Green catalog [PG], Kellerman et al. 1989). However, most optical quasar surveys are actively biased against finding red quasars. Since these surveys primarily search for UV-bright objects (e.g., Markarian, Lipovetsky, Markarian, & Stepanian 1987; PG, Schmidt & Green 1983; the Large Bright Quasar Survey, Hewett, Foltz, & Chaffee 1995; the Hamburg Quasar Survey, Engels et al. 1998), they are blind to red objects. As a result, optical bounds on how large a population of radio-quiet red quasars might exist are weak.

X-ray selection provides a way of selecting red quasars efficiently: hard X-rays (2–10 keV) penetrate even tens of magnitudes of optical extinction with minimal absorption. Even the lower energy band of *ROSAT* (0.5–2.5 keV) is not strongly affected by optical extinction of up to $\sim$2 mag.[2] Astrophysics might be against us, since although blue quasars are overwhelmingly X-ray loud (Avni & Tananbaum 1986), red ones might be intrinsically X-ray faint. Fortunately, however, radio-loud red quasars are known to be X-ray sources (Bregman et al. 1985; Elvis et al. 1994), so this is unlikely to be a problem.

[1] Also at Harvard-Smithsonian Center for Astrophysics, 60 Garden Street, Cambridge, MA 02138.

[2] For standard Milky Way composition and dust-to-gas ratio (Bohlin, Savage, & Drake 1978; Seaton 1979) the PSPC count rate is reduced by a factor of $1/e$ at $A_V = 1.7$ ($N_{\rm H} = 3 \times 10^{21}$ atoms cm^{-2}) for a power-law photon index of 2.0, all at 0 redshift.

Complete flux-limited X-ray surveys have found some red quasars or AGNs (Stocke et al. 1982; Kruper & Canizares 1989; Puchnarewicz et al. 1996, 1997). In particular the *ROSAT* International X-Ray/Optical Survey (RIXOS) survey (Puchnarewicz & Mason 1998) has identified a small sample of red quasars.

As part of a more general search for minority populations of X-ray sources, we have used the *ROSAT* (Trümper 1983) archive of pointed PSPC (Pfefferman et al. 1987) data to design an efficient search strategy explicitly targeting red quasars. The *ROSAT* pointed archive provides us with a tenfold increase in the number of X-ray sources from before *ROSAT* (to about 70,000) and reaches more than 10 times fainter than the *ROSAT* All-Sky Survey (Voges et al. 1996). By carefully selecting a small number of interesting objects, we can make an efficient search for a radio-quiet population of red quasars.

In this paper we find a substantial population of radio-quiet red AGNs on the quasar/Seyfert luminosity boundary.

2. SAMPLE SELECTION

Most *ROSAT* sources at high Galactic latitude are blue, unobscured AGNs (e.g., Boyle, Wilkes, & Elvis 1997; Schmidt et al. 1997). We use this fact to efficiently select *against* such objects and so isolate any red AGN that may be in the *ROSAT* archive.

As a compendium of the X-ray sources found by the *ROSAT* PSPC we have used the "WGACAT" catalog (which is named after its authors, White, Giommi, & Angelini 1995). This catalog was generated from *ROSAT* PSPC pointed observations using a sliding cell, detect algorithm. This method is sensitive to finding point sources but can also find spurious sources where extended emission is present. WGACAT includes a quality flag that notes such dubious detections based on a visual inspection of the fields. We have only used X-ray sources with high detection quality in order to exclude the spurious sources. From the WGACAT catalog we have selected sources by the following criteria:

1. X-ray bright ($f_X > 10^{-13}$ ergs cm^{-2} s^{-1}) to allow follow-up observations with other X-ray telescopes;
2. well detected with a signal-to-noise ratio greater than 10 and a WGACAT quality flag, DQFLAG, greater than 5;
3. within $r = 18'$ from the detector center to provide good positions;
4. at high galactic latitude ($|b| > 20°$) to minimize the fraction of Galactic stars (which are also red);
5. not within 2′ of the target position (at which point the source density reaches the background level) to select only random, serendipitous, sources;
6. north of decl. $= -18°$ in order to have two band measurements in the Automated Plate-measuring Machine (APM) catalog (McMahon & Irwin 1992), hence giving an archival optical color; and
7. unidentified, with WGACAT class $= 9999$ and no SIMBAD or NASA Extragalactic Database identification.[3]

The first six criteria selected 1624 sources. Since these sources were selected purely on their X-ray properties, they form a well-defined sample from which to study the incidence of minority X-ray populations, including any radio-quiet red quasars. Adding the requirement that a source be unidentified left 940 X-ray sources that could be examined for having red optical counterparts.

We then searched the APM catalog of objects detected on the Palomar Sky Survey for optical counterparts to the unidentified X-ray sources. To find counterparts, we used a search radius of 26″, which corresponds to about 95% confidence for X-ray sources within 18′ of the PSPC detector center (Boyle et al. 1995a). Of these, 881 sources had APM catalog counterparts brighter than the limiting magnitudes $O < 21.5$ and $E < 20$. (The remaining "blank" fields are the

[3] Although only "unidentified" sources were selected, one (1WGA J1118.0+4505; Table 1) turned out to be a known Seyfert 1 (Bade et al. 1995).

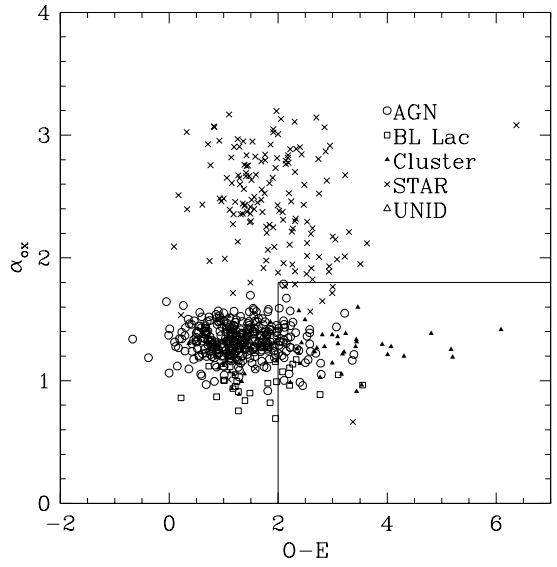

Fig. 1*a*

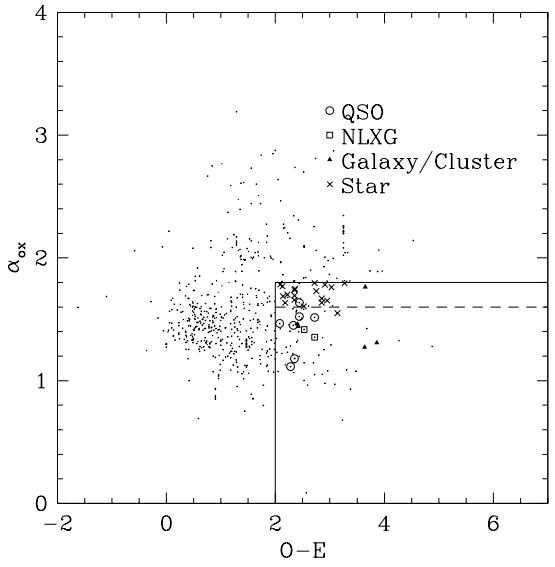

Fig. 1*b*

FIG. 1.—(*a*) Optically identified EMSS sources in the α_{ox}-$(O-E)$ plane. Different sources are marked by different symbols. Our source-selection criteria ($O-E > 2$, $\alpha_{ox} < 1.8$) are seen as a lower right box. (*b*) Same as (*a*) but for our *ROSAT* samples. The α_{ox} line shows how a slightly stricter criterion yields a larger fraction of red quasars.

subject of another study; Elvis, Kim, & Nicastro 1999.) Among these 881, many had only O-band magnitudes (suggesting that they are blue), leaving 575 with $O-E$ colors available.

The combination of the *ROSAT* X-ray flux and the APM magnitudes allows us to create a rough classification of the X-ray sources in our sample. The two Palomar O (blue) and E (red) magnitudes are close to Johnson B and Cousins R, respectively (Gregg et al. 1996). From the X-ray flux and the two optical magnitudes we can construct a two-color diagram of α_{ox}-$(O-E)$. α_{ox} is defined by the power-law index between 2 keV and 2500 Å (Tananbaum et al. 1979; Stocke et al. 1991). This diagram allows us to select red objects and then reduce the Galactic stellar population among these red objects by selecting the X-ray–loud population. Here we make use of the observation that in stellar sources the X-ray flux for a given optical flux is much weaker than in AGNs and clusters (e.g., Maccacaro et al. 1988). Figure 1*a* shows *Einstein* Extended Medium Sensitivity Survey (EMSS) X-ray sources (Stocke et al. 1991) in the α_{ox}-$(O-E)$ plane. This plot clearly illustrates the distinction between Galactic stellar sources and extragalactic sources.

Based on the EMSS source distribution, we divided the *ROSAT*-APM sources on the same plane (Fig. 1*b*). The $O-E$ APM colors are not as accurate as the EMSS values, which are based on CCD photometry. As a result, the spread of observed colors is wider (Fig. 1*b*), and there will be some blue objects in the red zone and vice versa. To create our list of red quasar candidates, we first excluded the 128 sources with $\alpha_{ox} > 1.8$, because they are likely to be Galactic stars. Then we excluded another 360 sources with blue colors, $O-E < 2$, because they are most likely just normal, blue, unobscured AGNs. This results in a final sample of 87 X-ray sources defined by the lower right corner of Figure 1*b* in the α_{ox}-$(O-E)$ plane.

Our sample of 87 optically red X-ray–loud sources is a mere 0.1% of the ~70,000 WGACAT sources. The fraction of X-ray sources that may be red quasars, however, is much larger: ~5% of the initial X-ray selected sample, ~15% of the unidentified sources with APM colors, and ~20% of X-ray bright objects with APM colors that will primarily be AGNs.

However, other classes of X-ray source than red quasars can inhabit this region of the α_{ox}-$(O-E)$ plane: for example, first-ranked elliptical galaxies in distant clusters of galaxies. Optical spectroscopy is needed to find red quasars. We have taken spectra for 51 of the 87 red quasar candidates, as is described in the next section.

3. OBSERVATIONS

3.1. *Optical Spectroscopy*

A typical X-ray error circle contains just 1–2 optical objects in the APM catalog. Since we have selected against blue counterparts, we began by observing the brightest red counterpart. If two objects were present, we aligned the spectrograph slit to obtain spectra of both at once. If this the first spectra did not find an AGN, we then observed the next faintest, if present. Since the density of (blue) AGNs at $B = 21$ is only ~0.005 per error circle (e.g., Zitelli et al. 1992), we expect only a 1 in 4 chance of AGN coincidence in the 51 spectra, so stopping once an AGN is found will not produce a significant number of false identifications.

We performed optical spectroscopy with the Multiple Mirror Telescope (MMT) on 1997 March 13–15, with the Fred Lawrence Whipple Observatory (FLWO) 60″ telescope on 1996 November 16–17 and 1997 February 12–13, and with the Cerro Tololo Inter-American Observatory (CTIO) 60″ telescope on 1997 February 3–5. We used long-slit apertures of 2″–3″ × 180″ and gratings with 300 gpm. The spectral resolutions are 6 and 9 Å for the MMT and 60″ telescopes, respectively. Wavelength coverage is about 3500–8000 Å. We took bias, dome flat, and twilight sky frames each night, and the corresponding corrections (bias subtraction, flat fielding, and illumination correction) were applied separately to each night of data. At least two standard stars were observed each night for spectrophotometric calibration. The observing conditions were not photometric, except for the CTIO run, so the absolute calibration is subject to a significant uncertainty. However, relative intensities (such as a line intensity ratio and an optical power-law index) are accurate within 20%, as is confirmed by multiple observations of the same source. Six sources are of undetermined nature because they are too faint and so gave spectra of too poor a signal-to-noise ratio.

3.2. *Classification of Spectra*

Of the 45 sources observed at a good signal-to-noise ratio, we have identified seven red quasars (Table 1). The results for these seven red quasars are presented in this paper. (The full data set will appear elsewhere.) The red quasars are mixed in with 18 stars and a small number of normal blue quasars, narrow emission line galaxies, and elliptical galaxies (Table 1). The elliptical galaxies are likely to be brightest cluster galaxies. We will report on these separately. For the remaining nine X-ray sources, the red optical candidate within the error circle turned out to be a star (mostly late type), but it is not likely that these red stars are the counterparts, because their α_{ox} values are too large for a star (see above; Maccacaro et al. 1988). The remaining optical candidates are not red, and hence we stopped making further observations. These nine sources and the three blue quasars measure the blue contamination of the sample and should not be considered as part of the list of red X-ray counterparts.

The optical spectra of the seven red quasars are shown in Figures 2*a* and 2*b*. Broad lines of Hα, Hβ, and Mg II are clearly seen in the spectra as well as bright narrow lines (e.g., [O III] λ5007), making the AGN character of the objects unambiguous. In Table 2 we tabulate source position, redshift, optical magnitude and color, X-ray flux and X-ray

TABLE 1

SUMMARY OF OPTICAL IDENTIFICATIONS OF RED X-RAY SOURCE COUNTERPARTS

Measurement	Total	Red Quasars	Too Faint	NLXG	Elliptical Galaxies	M Stars	Other Stars	Blue Quasars	Not Red
$1.8 > \alpha_{ox} > 1.6$ ($O \geq 19$).....	22	1	0	0	1	17	1	0	2
$\alpha_{ox} < 1.6$ ($O < 19$)	29	6	6	2	4	1	0	3	7
Total	51	7	6	2	5	18	1	3	9

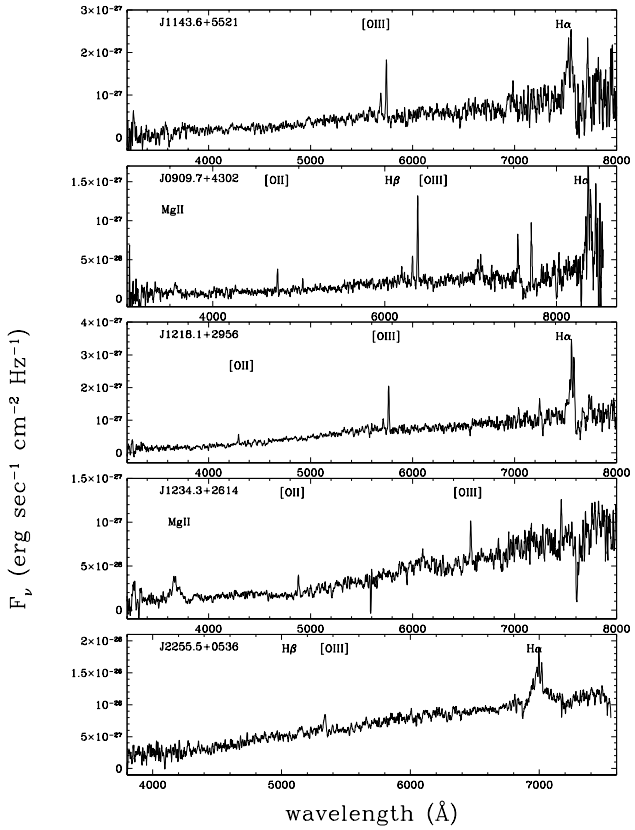

Fig. 2*a*

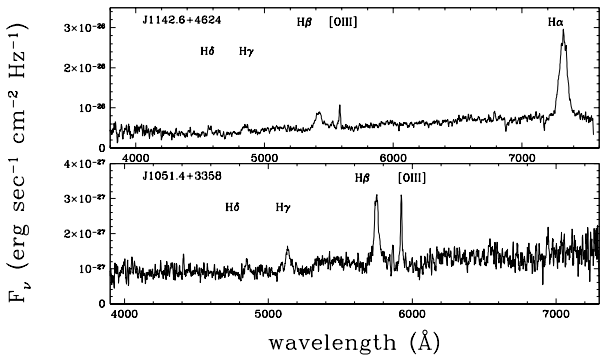

Fig. 2*b*

FIG. 2.—(*a*) Observed spectra of the five radio-quiet red quasars ($O-E > 2$ mag, $\alpha_{opt} > 2.0$). Broad lines such as Hα, Hβ, and Mg II are clearly seen in the spectra as well as bright narrow lines (e.g., [O III] λ5007). Those strong lines are marked in the figures. Steep continuum slopes and very weak Hβ line strengths indicate a significant amount of dust extinction ($A_V > 2$ mag), in contrast to (*b*), two quasar spectra with $\alpha_{opt} < 2.0$ and relatively strong Hβ lines.

colors, and α_{ox}, as well as offsets between the optical and X-ray positions.

In Figure 1*b* each class of identified sources is plotted in the α_{ox}-$(O-E)$ plane. The distribution of these sources can be compared with the EMSS sources in Figure 1*a*, confirming that most X-ray sources with low α_{ox} are indeed quasars or galaxy clusters. The selection technique finds 7/51 red quasars, i.e., 8% efficiency. A slightly stricter criterion, $\alpha_{ox} < 1.6$ (instead of 1.8), would have selected red quasars more efficiently (Table 2; Fig. 1*b*): only one M star (instead of 19 stars) would have been present, with only one red quasar lost, i.e., 6/29, a little over 20%. Of the initial 87, 71% (62) remain when $\alpha_{ox} = 1.6$ is the boundary.

3.3. *Observed Optical Properties of the Red Quasars*

We measured the optical continuum slopes by fitting a power law to the continuum spectra after excluding the strong emission lines (Table 3). Although all the sources

TABLE 2

BASIC PROPERTIES OF RED QUASARS

Name	Right Angle[a]	Declination[a]	Offset[b]	z	f_X[c]	α_{soft}[d]	α_{hard}[e]	O	$O-E$	α_{ox}
				($\alpha_{opt} < -2.0$)						
J2255.5+0536.....	22 55 31.0	05 36 01	11.3	0.0647	7.74	1.459	0.750	16.38	2.44	1.636
J1234.3+2614.....	12 34 21.8	26 13 28	5.0	0.3120	2.42	0.860	1.711	20.55	2.35	1.180
J1218.1+2956.....	12 18 07.1	29 55 21	4.3	0.1514	1.62	0.959	1.512	19.16	2.08	1.466
J0909.7+4302.....	09 09 43.6	43 02 47	7.0	0.2748	1.65	0.859	1.417	21.38	2.28	1.114
J1143.6+5521.....	11 43 35.5	55 20 21	4.0	0.1467	1.52	0.535	1.040	19.33	2.33	1.451
				($-0.9 > \alpha_{opt} > -2.0$)						
J1051.4+3358.....	10 51 28.3	33 58 04	8.0	0.1829	2.76	1.290	1.295	18.27	2.72	1.515
J1142.6+4624.....	11 42 41.2	46 24 21	3.1	0.1151	15.75	0.926	1.263	16.33	2.44	1.522

[a] Optical coordinate in Equinox J2000.
[b] Difference of X-ray and optical positions in arcseconds.
[c] In units of 10^{-13} ergs^{-1} cm^{-2}.
[d] X-ray spectral index in 0.1–0.8 keV.
[e] X-ray spectral index in 0.8–2.0 keV.

TABLE 3

LINE, CONTINUUM PROPERTIES, AND LUMINOSITIES OF RED QUASARS ADD D4000?

Name	α_{opt} [a]	Hα FWHM	Hα f [c]	Hα L [d]	M(O)	M(E)	$L(X)_{43}$ [b]
($\alpha_{opt} < -2.0$)							
J2255.5+0536.....	−2.39	5962	29.8	0.54	−21.6	−24.1	1.02
J1234.3+2614.....	−2.64	7184[e]	5.1[e]	2.70[e]	−21.1	−23.5	8.19
J1218.1+2956.....	−2.36	5011	5.2	0.56	−20.8	−22.9	1.21
J0909.7+4302.....	−2.43	2178	2.3	0.91	−20.0	−22.3	4.29
J1143.6+5521.....	−2.11	3223	5.1	0.51	−20.5	−22.9	1.07
($-0.9 > \alpha_{opt} > -2.0$)							
J1051.4+3358.....	−0.93	1797[f]	7.1[f]	7.10[f]	−22.1	−24.8	3.07
J1142.6+4624.....	−1.41	3104	81.3	4.90	−23.0	−25.4	6.75

[a] Optical spectral index, $f_\nu \propto \nu^{\alpha_{opt}}$.
[b] In units of 10^{43} ergs s^{-1}.
[c] In units of 10^{-15} ergs cm^{-2} s^{-1}.
[d] In units of 10^{43} ergs s^{-1}.
[e] Mg II.
[f] Hβ.

were selected based on a red $O-E$ color, in some cases the observed optical continuum shape is relatively flat. This is because of both line emission contributing to the blue and/or red bands and uncertainties on the O and E magnitudes, particularly when the object is faint (M. Irwin 1996, private communication). The power-law index ($F_\nu \sim \nu^{\alpha_{opt}}$) ranges from −0.9 to −2.6. A steep optical continuum, $\alpha_{opt} < -2$, is found in five of the seven red quasars, while even the remaining two, intermediate red quasars are redder ($-1.5 < \alpha_{opt} < -1$) than is found for UV-excess–selected quasars (-0.2 ± 0.8; Neugebauer et al. 1987). To illustrate the spectral differences between these two groups, we display the spectra separately in Figures 2*a* (steep) and 2*b* (intermediate).

In addition to the difference in continuum shape, these two groups also differ in their Hβ line strengths (see Figs. 2*a* and 2*b*). The group with the steep optical continuum have only weak Hβ lines or no detection, whereas the group with a relatively flat continuum have stronger Hβ lines. Since the ratio of Hα to Hβ is sensitive to optical extinction, this suggests more reddening in the steep slope group than the intermediate slope group (Table 3), which is in accord with the optical continuum slopes.

To quantify this effect for those quasars with no detected Hβ line, we estimated its upper limit using a simple method that assumes a box profile with a base equal to 3000 km s^{-1} (the mean FWHM of detected Hβ lines) and a height equal to 3 times the fluctuation noise on the continuum. This is a conservative measurement, because the peak of a Gaussian profile would be more easily detected than the flat top of a box profile, particularly when the line width is considerably larger than the spectral resolution. Monte Carlo simulations using a Gaussian line profile assuming Poisson statistics show that the box profile overestimates the upper limit by up to 50% for the adopted line width, while it reproduces consistent results when the line width is comparable with the spectral resolution. For the two objects whose optical spectra do not cover the Hα line, we have instead used the [O III]/Hβ ratio as a measure of relative Hβ strength.

For all five quasars with $\alpha_{opt} < -2$, the Hα/Hβ ratios are greater than 5, while the [O III]/Hβ > 0.8. The line ratios of the two remaining quasars are smaller (Table 2), which is consistent with less reddening in intermediate-slope objects.

None of the characteristic galaxian stellar absorption features[4] are seen in our spectra. Most strikingly, no 4000 Å break is seen in any of the five red quasars for which our spectra cover that region, including all of the steep-slope group. Typical values of $D(4000)$[5] are 1–1.2, as is expected from the measured optical slopes. These compare with values of 2 ± 0.2 for normal E and S0 galaxies Dressler & Shectman (1987). Hence any starlight continuum contribution to the red quasar continuum must be minor.

3.4. *X-Ray Colors of the Red Quasars*

To determine the rough X-ray spectral properties of the seven red quasars, we first double-checked in the PSPC images that the sources were cleanly separated from any confusing sources, then measured their X-ray hardness (HR = H/M) and softness (SR = S/M) ratios based on the count rates in the standard *ROSAT* PSPC bands: soft, S (0.1–0.4 keV); medium, M (0.4–0.86 keV); and hard, H (0.87–2 keV). These ratios are then converted to effective X-ray spectral indices, α_{soft} and α_{hard} (Table 2), to correct for the variable Galactic line-of-sight absorption and the energy-dependent point-spread function. (These are not physical slopes but should be considered analogous to $U-B$ and $B-V$ colors; see Fiore et al. 1998 for a detailed discussion of the estimation and usage of effective X-ray spectral indices.) Due to the low signal-to-noise ratio of X-ray data, individual spectral indices are not reliable. However, the locus of their colors forms a useful indicator of global X-ray properties.

We compare the colors of the red quasars with those of normal radio-quiet quasars in Figure 3. The large filled symbols are the red quasars reported here, while the cloud of small dots represents radio-quiet quasars from the sample of Fiore et al. (1998). On average, the red quasars have smaller α_{soft} than α_{hard}, indicating a cutoff spectral shape. [The line pairs around the periphery of the figure

[4] CH *G*-band λ4304, Mg I λ5175, Ca + Fe λ5269, Na λλ5890, 5896.
[5] $D(4000) = F_\nu(4050–4250\ \text{Å})/F_\nu(3750–3950\ \text{Å})$, Dressler & Shectman (1987).

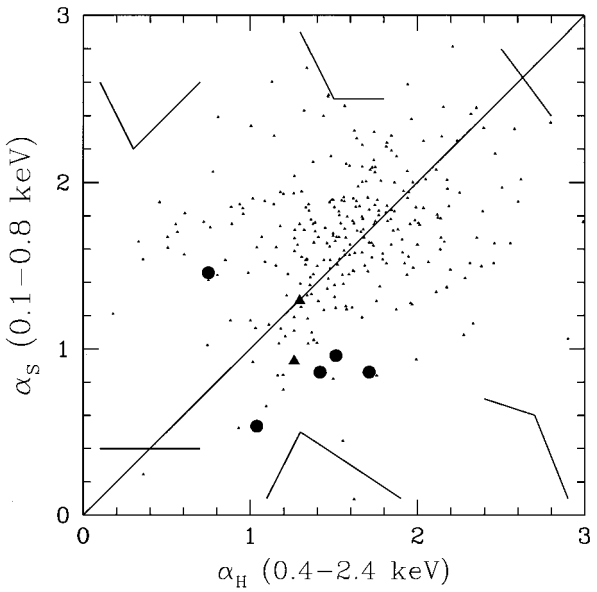

FIG. 3.—Effective soft and hard *ROSAT* PSPC X-ray spectral indices (see text) of the red quasars (*large filled symbols*) compared with normal radio-quiet quasars (*small dots*; Fiore et al. 1998). Steep–optical spectrum ($\alpha < -2$) red quasars are shown as circles, and intermediate–optical spectrum ($-1.5 < \alpha < -1$) red quasars are shown as triangles. The line pairs around the periphery of the figure show outline spectral shapes for their locations in the (α_{hard}, α_{hard}) plane.

show outline spectral shapes for their locations in the (α_{soft}, α_{hard}) plane.] This is consistent with their having the moderate X-ray absorption expected from their optical properties (Fiore et al. 1998).

4. DISCUSSION

These observations show that a population of red AGNs can be extracted efficiently from the *ROSAT* pointed archive. Moreover, the red AGNs we find are radio quiet. None of them is a radio source in the NRAO VLA Radio Sky Survey ($f_{1.4GHz} < 2.5$ mJy; Condon et al. 1998), implying $R_L = \log [f(\text{opt})/f(5\text{ GHz})] < 2.0$, compared with $2 < R_L < 5$ for radio-loud quasars (Wilkes & Elvis 1987). The agreement of X-ray colors, optical continuum slope, and Hα/Hβ ratios with the same value of obscuring dust and gas ($A_V \sim 1$–2) argues for their being dust reddened objects rather than instrinsically red continua.

Puchnarewicz & Mason (1988) discuss a similar population of 14 candidate red, $\alpha_{opt} > 2$, AGNs derived from the RIXOS sample, which extends to several times fainter X-ray fluxes. The RIXOS sample was selected from the *ROSAT* pointed archive based on X-ray flux alone. (There is one object in common between the two samples.) Two of the red RIXOS AGNs may be intrinsically red, and three have clear reddening. So there is currently a total of eight reddened AGNs available from *ROSAT*.

The red AGNs, both from this sample and from RIXOS, are borderline quasar/Seyfert objects. The observed optical luminosities of the red AGNs are modest, lying at the high end of the traditional Seyfert luminosity range ($M_B > -23$ mag; Veron-Cetty & Veron 1984; Schmidt & Green 1983): from $M_O = -20$ to -22 mag.[6] The dereddened, intrinsic luminosity of the sources is likely to be significantly higher, depending on the amount of absorption (the lower limit on the extinction is 2–3 mag in O). This places them at $-25 < M_O < -22$, which is within the quasar regime. Similarly, the observed X-ray luminosity ranges from 1.3×10^{43} to 1.2×10^{44} ergs s^{-1}, while the intrinsic luminosities are likely to be higher by about a factor of 2, depending on the intrinsic spectrum and the amount of absorption present.

The precise allocation of these AGNs as quasars or Seyferts is not fundamentally very interesting, since this is just a conveniently chosen value on a continuous luminosity scale. For simplicity we will refer to them as red quasars for the rest of this paper. It is, however, interesting to understand why much more or much less luminous AGNs were not found in the two red quasar searches. Is this a selection effect, or is there a physical preference for red objects to cluster in a limited range of luminosity? We will return to this question later (§ 4.3).

The existence of a red quasar population immediately raises important questions. What makes them red compared with usual blue quasars? How common are they, particularly once allowance is made for their reduced flux due to probable obscuration? If they are absorbed, by how much? Where is the absorbing dusty material? Might a larger, more obscured, AGN population exist?

4.1. *How Common are Red Quasars?*

We can address the relative numbers of red quasars in a rough way. The population, although a minority, is quite common. We found seven red quasars out of 45 candidates for which our spectroscopy was adequate to produce a classification. Assuming that the 45 were a random subsample of the original sample of 87, that sample would produce 14 red quasars. This is 2.4% of 575 sources with optical colors available. At our flux limit, Stocke et al. (1991) find that 51% of all X-ray sources are AGNs. So a minimum of 13.5/288 (4.7%) AGNs in our unidentified sample are radio-quiet red quasars (with $O < 20$) at this soft X-ray flux level. The Boyle & di Matteo (1995) upper limit of 9% of Cambridge *ROSAT* Serendipity Survey (CRSS) X-ray sources being red quasars is consistent with the minority population of moderately obscured ($A_V = 2$) quasars we have found here.

Additional red quasars could be hidden in our sample. Our sample of 45 classified spectra is not a random subsample of the candidate list. Figure 1*b* shows that we preferentially selected objects with $\alpha_{ox} > 1.3$, i.e., the brighter objects (with $B < 21.5$). If the six objects for which we attempted to get spectra turn out to be red quasars, then the fraction of red quasars among the PSPC AGNs could be almost double our first estimate. There are a further 36 red candidates for which no spectroscopy was attempted. So the true occurrence rate of red quasars is uncertain by a factor of 7.

To find the fraction of red quasars among all the AGNs in our X-ray, flux-limited sample, we must allow for the 165–300 blue AGNs in the identified sample, so 1%–7% of the whole soft X-ray AGN population is red.

If the red AGNs are obscured, then the intrinsic rate of occurrence of red quasars has to be calculated relative to their unreddened parent population. Obscuration by $A_V = 2$ reduces their unobscured X-ray fluxes by a factor of ~ 2. Since higher flux AGNs are rarer (the X-ray–selected AGN

[6] We have used $H_0 = 50$ km s^{-1} Mpc^{-1} and $q_0 = 0$.

log N/log S relation has a slope of $-3/2$ in this flux range; Hasinger 1995; Della Cecca et al. 1992), the red population forms a larger fraction of this population, $\sim 3\%$–20%.

Using the fraction of the sources at the intrinsic flux of the red quasars allows us to compare our result with samples unaffected by obscuration and with model predictions. Comparisons with the observed frequency of radio-loud red quasars with broad emission lines found by Smith & Spinrad (1980; 178 MHz 3CR) and Stickel et al. (1996; 5 GHz 1 Jy sample) and with the Comastri et al. (1995) predictions are straightforward.

Red quasars are found in 15% of the 3CR source sample and 6%–20% of the 1 Jy (Carilli et al. 1998) sample. These are comparable with the 3%-20% of the "intrinsic flux" X-ray population that we find, suggesting that the radio-loud and radio-quiet quasar populations have similarly sized populations of moderately obscured quasars. The obscuration in the 3CR red quasars is also about $A_V = 2$ (Elvis et al. 1994; Economou et al. 1995; Rawlings et al. 1995). For four objects in the 1 Jy sample, Carilli et al. (1998) estimate lower limits on A_V from 2 to 5 based on extrapolating the radio-infrared index to the optical. However, since such steeply rising slopes are not known among unobscured quasars, these limits are likely to be too large, and values comparable with the 3CR estimates are probably acceptable.

For AGNs with $N_{\rm H} < 10^{22}$ cm^{-2}, the Comastri et al. (1995) model predicts that 26% will have $10^{21} < N_{\rm H} < 10^{22}$ cm^{-2} ($A_V \sim 2$), which is somewhat larger but comparable with the numbers found here. Comastri et al. predict far larger numbers of more obscured objects.

4.2. *More Obscured Objects*

More obscured objects may exist. Puchnarewicz & Mason (1998) find several objects with steeper optical continua, and Figure 1*b* shows several redder candidates and many more X-ray loud candidates with no optical spectra to date. Webster et al. (1995) suggested that $A_V = 5$ may be typical of their red objects, giving their putative *ROSAT* counterparts in our sample $V = 23$–25, which is below the Palomar Sky Survey limit. $A_V = 5$ corresponds to a column of 9×10^{21} atoms cm^{-2}, which would reduce *ROSAT* PSPC count rates to 15% of their unobscured values. These objects would then be hidden as a 6% minority among the more common, lower luminosity, unabsorbed quasars if they had the same *unobscured* space density as normal blue quasars. Some 9% of our initial X-ray–selected sample are "blank field" objects, i.e., have no counterpart on the Palomar Sky Surveys. A fraction of these could be more heavily obscured red quasars. Boyle & di Matteo (1995) find that the CRSS sample could be missing no more than 9% (at the observed flux) in red quasars. Subtracting the 1% of moderately obscured quasars we have identified still leaves 8% that could be highly obscured. Hence the CRSS result is, perhaps surprisingly, consistent with a sizeable, heavily obscured population. The Comastri et al. (1995) model predicts a comparable population of AGNs with $N_{\rm H} \sim 10^{22}$ cm^{-2}, which is 1.1 times larger than the unobscured population.

In our sample the occurrence of red quasars appears to be 4 times higher for $O > 19$ mag (4/12) than for $O < 19$ mag (3/32; Table 2), although the number of sources is small. Such a trend is expected if the quasars are heavily absorbed. An increase in $N_{\rm H}$ from 3×10^{21} to 1×10^{22} cm^{-2} cuts the *ROSAT* flux by a factor of 2.4 but reddens the V band by 3.8 mag (a factor 33). So the optically fainter sources might well be redder. However, the RIXOS red quasars (Puchnarewicz & Mason 1998) show no correlation of optical slope with m_V : the three steepest slopes are all in the brighter half of the sample of 14. Gunn & Shanks (1998) have pointed out that while redshifting the ultraviolet into the optical increases the effects of reddening, the corresponding shift of hard X-rays into the soft *ROSAT* band *decreases* the effectiveness of reddening.

To estimate an accurate fraction of this potential hidden population needs a larger sample, including more absorbed, fainter objects. At even larger column densities (10^{23}–10^{24} cm^{-2}) the Comastri et al. (1995) model predicts nearly 4 times the unobscured population. More heavily obscured quasars could be found in hard X-ray surveys from *ASCA* (Ueda et al. 1998) and the *Beppo-SAX* HELLAS survey (Fiore et al. 1999).

4.3. *Limited Luminosity Range*

It is striking that while *ROSAT* surveys that are defined simply by an X-ray flux limit find AGNs spanning over 3 decades in X-ray luminosity (e.g., CRSS, Boyle et al. 1997; RIXOS, Puchnarewicz et al. 1996), both RIXOS and this survey find red quasars in only 1 decade of luminosity, and this decade is the lowest one in which RIXOS and CRSS AGNs are found. A two-tail Kolmogorov-Smirnov test shows that the chance that red and nonred AGNs from RIXOS come from the same luminosity distribution is only $\sim 2\%$. This suggests that predominantly lower luminosity AGNs are obscured. (Note that the observed amount of obscuration only decreases the observed X-ray luminosity by a factor of ~ 2, and so does not itself cause the low observed luminosities.)

Similar suggestions have been made before: Lawrence & Elvis (1982) found that only AGNs below $L_{\rm X} \sim 10^{44}$ ergs s^{-1} (2–10 keV) showed obscuration. Occasional examples of highly obscured type 2 (i.e., narrow-line) quasars have been reported (Stocke et al. 1982; Almaini et al. 1995; Shanks et al. 1995), and careful searches have found broad Hα in most cases (Halpern, Eracleous, & Forster 1998), making them similar to the red quasars found here. Searches among the fainter objects in our sample and searches at higher energies (e.g., the *Beppo-SAX* HELLAS survey; Fiore et al. 1999) will be more effective at finding a high-luminosity red quasar population.

The Comastri et al. X-ray background models assume luminosity functions for the obscured objects that are identical to those of the unobscured objects except for normalization and so predicts high-luminosity red quasars. If instead obscured AGNs occur preferentially at low luminosity, this will substantially affect the model predictions. We would, for example, expect the obscured population to be more numerous and at lower redshift.

If there is a real deficit of high-luminosity red quasars, then one possibility to explain this lack might have been that as an AGN became more luminous, the continuum ionized the obscuring medium, rendering it transparent to X-rays. However, ionized absorbers are also more common at lower luminosities (Laor et al. 1994). So most likely, high-luminosity AGNs have fewer lines of sight with intervening material regardless of ionization state. (Interestingly, this is in the same sense as the Baldwin effect: that higher luminosity quasars have weaker C III] λ1909 emission lines.) Any

physical model of a quasar would need to explain this difference.

4.4. *Physical Properties*

We can say only a little about the physical properties of the red quasars from this data.

The consistency of the optical reddening indicators with the X-ray colors suggests that the same obscuring material covers both emitting regions and that it lies outside the broad emission line region.

Smith & Spinrad (1980) suggested that the redness of the red 3CR quasars is intrinsic to the continuum emission process based on the lack of an absorption feature at $\lambda = 2200$ Å, which is a typical characteristic of Milky Way dust (e.g., Bless & Savage 1972). The detection of 21 cm H I absorption toward a large fraction of the 1 Jy (Stickel et al. 1996) red quasars (Carilli et al. 1998) argues for dust reddening in those objects. Since our sample of radio-quiet quasars is relatively nearby (with redshifts up to 0.3), we cannot check for this feature directly. However, this explanation is in contrast to the observed Balmer decrement and the X-ray colors. It is possible that the reddened 3CR sources contain dusty, ionized absorbers, as is seen in 3C 212 (Mathur 1994; Elvis et al. 1994) and IRAS 17020+4544 (Komossa & Bade 1998), where the dust composition may differ depending on, for example, the quasar continuum shape. Ultraviolet observations are needed to investigate the $\lambda = 2200$ Å feature but are probably infeasible at present.

4.5. *Other Red AGNs*

Some previous studies have considered red AGN-like objects in X-ray surveys. The RIXOS survey (Puchnarewicz & Mason 1998) found that 9% (14/160) of their AGNs were red. However, only three of the RIXOS sources have Balmer decrements that require reddening, so the true occurrence rate of reddened objects may be similar to what we have found. The fainter flux limit of the RIXOS survey may render more absorbed objects visible. Certainly, the steeper optical slopes ($-2.5 > \alpha_{\rm opt} > -4.0$) of half the RIXOS sample suggest greater reddening.

Kruper & Canizares (1989) studied red AGNs in *Einstein* X-ray–selected samples and indirectly concluded that these are red because of the presence of host galaxies. Benn et al. (1998) arrive at a similar conclusion for low-frequency, selected radio-loud quasars. However, no galaxian starlight features are seen in our spectra, and the host galaxy cannot explain the observed Balmer decrements in our sample. The Kruper & Canizares objects are not as red as our samples, having $B-I = 1.5$–2.5 mag. If we take $R-I$ to be 0.5–1.0 mag (this is the $R-I$ range of the samples in their Table 2), $B-R$ would be less than 2.0, our defining threshold. In fact, none of their objects with measured R magnitudes exceed $B-R = 2.0$.

The narrow-line X-ray galaxies (NLXGs) found plentifully in deep *ROSAT* surveys (e.g., Boyle et al. 1995a) are also normally assumed to be obscured AGNs (e.g., Hasinger et al. 1998; Schachter et al. 1998). X-ray–absorbed NLXGs could contribute significantly to the cosmic X-ray background if they are more common at fainter X-ray flux levels, as was suggested by McHardy et al. (1998; see also Hasinger et al. 1998 for a cautionary note). Although they have similar X-ray luminosities to the NLXGs, the X-ray–selected red quasars are not simply the same population, however. The red quasars have the normal, broad optical emission lines of quasars, while NLXGs have either none or only extremely weak ones (Boyle et al. 1995b; Figs. 2*a* and 2*b*). Moreover, NLXGs usually exhibit blue optical continua (for example, $O-E < 2$ for five out of six NLXGs in CRSS; Boyle et al. 1997), while red quasars have red optical continua ($O-E > 2$). Further X-ray and optical study of these objects may let us understand whether they are two separate populations or are related by, e.g., special viewing geometry or scattering of a blue continuum.

The Palomar survey of the nuclei of bright galaxies (Ho, Filippenko, & Sargent 1997) is based on a sample of galaxies selected for their nonnuclear properties and so is less biased against finding red AGNs than most other optical search methods. The Palomar AGNs are low-luminosity AGNs, allowing us to see whether the high incidence of red AGNs at lower luminosities continues to increase at even lower values. The Palomar survey finds that 18% (8/44) of Seyfert nuclei have $A_V > 2$ based on their narrow-line Balmer decrements (Ho et al. 1997). However, almost all of these are LINERs or type 2 Seyferts, which may have large reddening toward the broad-line region. Only one Seyfert (NGC 7479) shows any evidence for a broad-line component. Broad emission lines are extremely hard to detect at these flux levels, but the suggestion is that the middling luminosities toward the quasar/Seyfert borderline are particularly prone to moderate obscuration.

5. CONCLUSIONS

Radio-quiet red quasars can be found in substantial numbers. They comprise at least 1%, and potentially 7%, of the soft X-ray population in a flux limited survey. Correcting the X-ray fluxes to their intrinsic values puts them among brighter AGNs, where they form 3% of the population. Allowing for blank field sources, as much as 20% of *ROSAT* selected quasars may be red at a given unobscured flux. The size of this population is consistent with previous upper limits, with the Comastri et al. (1995) model for the X-ray background, and with the size of the radio-loud 3CR and 1 Jy red quasar populations. Red quasars seem to be preferentially lower luminosity objects on the quasar/Seyfert borderline but not at higher or lower luminosities. Such a bias against obscured high-luminosity objects would affect X-ray background estimates for this population and would need explaining in a physical model of quasars.

We stress that the quasars we find have broad optical lines. They are not NLXGs, which by contrast have predominantly narrow optical permitted lines and blue continua.

The optical slopes, Hα/Hβ ratios, and X-ray colors are all consistent, with reddening by $A_V \sim 2$ assuming standard Milky Way dust properties. So the same obscuring material probably covers each of the emitting regions.

A significant population of more highly obscured ($A_V = 5$) quasars could well exist and be consistent with the results here, with earlier *ROSAT* limits, and would be as predicted by the Comastri et al. (1995) model. Hard X-ray surveys will soon settle the question of the size of any such population.

Using a minor refinement of the technique presented here, red quasars can be found with high (20%) efficiency in the *ROSAT* data.

We thank L. Angelini for helping us to use WGACAT and M. Irwin for use of the APM online catalog. We also

thank F. Fiore and F. Nicastro for providing their program to calculate X-ray spectral indices and F. Fiore once again for supplying the X-ray slopes of the radio-quiet sample in Figure 3. The support by the FLWO, MMT, and CTIO staffs in setting up and operating various instruments were invaluable to this study. The HEASARC/GSFC PIMMS program was used to calculate PSPC count rates. This work was supported by NASA grants NAG5-3066 (ADP), NAG5-6078 (LTSA), and NASA contract NAS8-39073 (ASC).

REFERENCES

Almaini, O., Boyle, B. J., Griffiths, R. E., Shanks, T., Stewart, G. C., & Georgantopoulos, I. 1995, MNRAS, 277, L31
Avni, Y., & Tananbaum, H. 1986, ApJ, 305, 83
Bade, N., Fink, H. H., Engels, D., Voges, W., Hagen, H.-J., Wisotzki, L., & Reimers, D. 1995, A&AS, 110, 469
Benn, C. R., Vigotti, M., Carballo, R., Gonzalez-Serrano, J. I., & Sánchez, S. F. 1998, MNRAS, 295, 451
Bless, R. C., & Savage, B. D. 1972, ApJ, 171, 293
Bohlin, R. C., Savage, B. D., & Drake, J. F. 1978, ApJ, 224, 132
Boyle, B. J., & di Matteo, T. 1995, MNRAS, 277, L63
Boyle, B. J., McMahon, R. G., Wilkes, B. J., & Elvis, M. 1995a, MNRAS, 285, 511
———. 1995b, MNRAS, 276, 315
Boyle, B. J., Wilkes, B. J., & Elvis, M. 1997, MNRAS, 285, 511
Bregman, J. N., Glassgold, A. E., Huggins, P. J., & Kinney, A. L. 1985, ApJ, 291, 505
Carilli, C. L., Menten, K. M., Reid, M. J., Rupen, M. P., & Yun, M. S. 1998, ApJ, 494, 175
Comastri, A., Setti, G., Zamorani, G., & Hasinger, G. 1995, A&A, 296, 1
Condon, J. J., Cotton, W. D., Greisen, E. W., Yin, Q. F., Perley, R. A., Taylor, G. B., & Broderick, J. J. 1998, AJ, 115, 1693
Della Ceca, R., Maccacaro, T., Gioia, I. M., Wolter, A., & Stocke, J. T. 1992, ApJ, 389, 491
Dressler, A., & Shectman, S. A. 1987, AJ, 94, 899
Economou, F., Lawrence, A., Ward, M. J., & Blanco, P. R. 1995, MNRAS, 272, L5
Elvis, M., Fiore, F., Mathur, S., & Wilkes, B. J. 1994, ApJ, 425, 103
Elvis, M., Kim, D.-W., & Nicastro, F. 1999, in preparation
Engels, D., Hagen, H.-J., Cordin, L., Koehler, S., Wisotzki, L., & Reimers, D. 1998, A&AS, 128, 507
Fiore, F., Elvis, M., Giommi, P., & Padovani, P. 1998, ApJ, 492, 79
Fiore, F., LaFranca, F., Giommi, P., Elvis, M., Comastri, A., Matt, G., & Molendi, S. 1999, in preparation
Gregg, M. D., Becker, R. H., White, R. L., Helfand, D. J., McMahon, R. G., & Hook, I. M. 1996, AJ, 112, 407
Gunn, K. F., & Shanks, T. 1998, Astron. Nachr., 319, 66
Halpern, J. P., Eracleous, M., & Forster, K. 1998, ApJ, 501, 103
Hasinger, G. 1995, in MPE Rep. 263, Röntgenstrahlung from the Universe, ed. H. U. Zimmermann, J. Trümper, & H. Yorke (Garching: MPE), 291
Hasinger, G., Burg, R., Giacconi, R., Schmidt, M., Trümper, J., & Zamorani, G. 1998, A&A, 329, 482
Hewett, P. C., Foltz, C. B., & Chaffee, F. H. 1995, AJ, 109, 1498
Ho, L. C., Filippenko, A., & Sargent, W. L. W. 1997, ApJS, 112, 315
Kellerman, K. I., Sramek, R., Schmidt, M., Shaffer, D. B., & Green, R. 1989, AJ, 98, 1195
Kollgaard, R. I., Feigelson, E. D., Laurent-Muehlson, S. A., Spinrad, H., Dey, A., & Brinkmann, W. 1995, ApJ, 449, 61
Komossa, S., & Bade, N. 1998, A&A, 331, L49
Kruper, J. S., & Canizares, C. R. 1989, ApJ, 343, 66
Laor, A., Fiore, F., Elvis, M., Wilkes, B. J., & McDowell, J. C. 1994, ApJ, 435, 611
Lawrence, A., & Elvis, M. 1982, ApJ, 256, 410
Lipovetzky, V. A., Markarian, B. E., & Stepanian, J. A. 1987, in Observational Evidence of Activity in Galaxies, ed. E. Ye. Khachikian, K. J. Fricke, & J. Melnick (Dordrecht: Reidel), 17
Maccacaro, T., Gioia, I. M., Wolter, A., Zamorani, G., & Stocke, J. T. 1988, ApJ, 326, 680
Mathur, S. 1994, ApJ, 431, L75
McHardy, I. M., et al. 1998, MNRAS, 295, 641
McMahon, R. G., & Irwin, M. J. 1992, in Digitized Optical Sky Surveys, ed. H. T. MacGillivray & E. B. Thomson (Dordrecht: Kluwer), 417
Neugebauer, G., Green, R. F., Matthews, K., Schmidt, M., Soifer, B. T., & Bennet, J. 1987, ApJS, 63, 615
Pfeffermann, E., et al. 1987, Proc. SPIE, 733, 519
Puchnarewicz, E. M., et al. 1996, MNRAS, 281, 1243
———. 1997, MNRAS, 291, 177
Puchnarewicz, E. M., & Mason, K. O. 1988, MNRAS, 293, 243
Rawlings, S., Lacy, M., Sivia, D. S., & Eales, S. A. 1995, MNRAS, 274, 428
Sandage, A. R. 1965, ApJ, 141, 1560
Sanders, D. B., et al. 1988, ApJ, 325, 74
Schachter, J. S., Fiore, F., Elvis, M., Mathur, S., Wilson, A. S., Morse, J. A., Awaki, H., & Iwasawa, K. 1998, ApJL, 503, L123
Schmidt, M., et al. 1997, A&A, 329, 495
Schmidt, M., & Green, R. F. 1983, ApJ, 269, 352
Seaton, M. J. 1979, MNRAS, 187, 785
Shanks, T., Almaini, O., Boyle, B. J., Done, C., Georgantopoulos, I., Griffiths, R. E., Rawling, S. J., & Stewart, G. C. 1995, Spectrum: Newsletter of the Royal Obs., 7, 7
Smith, H. E., & Spinrad, H. 1980, ApJ, 236, 419
Stickel, M., Rieke, G. H., Kühr, H., & Rieke, M. J. 1996, ApJ, 468, 556
Stocke, J. T., Liebert, J., Maccacaro, T., Griffiths, R. E., & Steiner, J. E. 1982, ApJ, 252, 69
Stocke, J. T., Morris, S. L., Gioia, I. M., Maccacaro, T., Schild, R., Wolter, A., Fleming, T. A., & Henry, J. P. 1991, ApJS, 76, 813
Tananbaum, H., et al. 1979, ApJ, 234, L9
Trümper, J. 1983, Adv. Space Res., 2:4, 241
Ueda, Y., et al. 1998, Nature, 391, 866
Véron-Cetty, M.-P., & Véron, P. 1984, ESO Special Rep. 1
Voges, W., et al. 1996, IAU Circ., 6420, 2
Webster, R. L., Francis, P. J., Peterson, B. A., Drinkwater, M. J., & Mascl, F. J. 1995, Nature, 375, 469
White, N., Giommi, P., & Angelini, L. 1995, WGACAT, http://heasarc.gsfc.nasa.gov/W3Browse/all/wgacat.html
Wilkes, B. J., & Elvis, M. 1987, ApJ, 323, 243
Zitelli, V., Mignoli, M., Zamorani, G., Marano, B., & Boyle, B. J. 1992, MNRAS, 256, 349